Prediction of Failure Pressure for Defective Pipelines Reinforced with Composite System, Accounting for Pipe Extremities

S. Budhe, M. Banea, Silvio DE BARROS

Prediction of failure pressure for defective pipelines reinforced with composite system, accounting for pipe extremities

S. Budhe[1*], M. D. Banea[1], S. de Barros[1,2]

[1]CEFET/RJ, Federal Center of Technological Education of Rio de Janeiro, Av-Maracanã, 229, 20271- 110, Rio de Janeiro/RJ, Brasil

[2]Université de Nantes, Institut de Rechercheen Génie Civil et Mécanique, Saint-Nazaire, France

M. D. Banea, mdbanea@gmail.com

S. de Barros, silvio.debarros@gmail.com

S. Budhe, sandipiit@gmail.com

Abstract:

The present paper is concerned with the failure analysis of the wall loss defect in pipelines reinforced with a polymer based composite repair system. The main goal is to propose a methodology with accounting for the pipe extremities (axial stress) in an analysis to predict an accurate failure pressure. The proposed methodology defines a simple expression for a real test specimen condition (closed cap cylinder), which allows to estimate the failure pressure using the elastic properties of the materials and test specimen geometry. Hydrostatic tests performed in different laboratories are used to validate the proposed methodology. The results show a good agreement between the model prediction and the experimental failure pressure results in all cases. However, a careful selection of the remaining strength factor is needed, as it impacts on the accuracy and conservative level of the failure pressure. In addition to the axial stress, there is a possibility to refine the theoretical prediction of the failure pressure value by accounting for the plastic deformation far from the defect region as well as the radial stress in the failure analysis.

Keywords: Failure pressure; axial stress; corroded metallic pipelines; hydrostatic test; composite repair systems

Nomenclature:

P_i	Internal pressure (MPa)	E_{sleeve}	Young's modulus of the composite sleeve (MPa)
P_f	Failure pressure (MPa)	E_{rr}	Young's modulus of the composite in the radial direction (MPa)
P_c	Contact pressure between the steel pipe and composite (MPa)	$E_{\theta\theta}$	Young's modulus of the composite in the circumference direction (MPa)
r_i	Internal radius of steel pipe (mm)	σ_θ	Circumferential stress in pipe (MPa)
r_o	External radius of steel pipe (mm)	ε_θ^p	Plastic strain
r_e	External radius of composite repair (mm)	ε_θ^e	Elastic strain
e_{pipe}	Pipe thickness (mm)	σ_y	Yield stress of the pipe (MPa)
e_{sleeve}	Composite repair thickness (mm)	σ_{ult}	Ultimate stress of the pipe (MPa)
α_θ	Remaining strength factor	σ_{flow}	Flow stress of the pipe (MPa)
L	Defect length (mm)	K, N	Material constant for plastic characterization
w	Width of defect section (mm)	$\nu_{r\theta}$	Poisson's ratio
D	External diameter of the pipe (mm)	σ_r	Radial stress in the pipe (MPa)
d	Depth of defect (mm)	σ_z	Axial stress in the pipe (MPa)
E_{pipe}	Young's modulus of the pipe (MPa)	$\tau_{r\theta}$	Shear stress in the r-θ plane (MPa)
u_r	Radial displacement (mm)	$\tau_{\theta z}$	Shear stress in the θ-z plane (MPa)
P_{max}^{th}	Maximum theoretical failure pressure (MPa)	τ_{rz}	Shear stress in the r-z plane (MPa)
P_{max}^{exp}	Maximum experimental failure pressure (MPa)	M_t	Bulging factor
σ_1 σ_2 σ_3	Principal stresses along the 1, 2 and 3 directions	e	Cylinder thickness

1. Introduction

In recent years, it has been observed a rapid growth of the use of polymeric composite materials to repair metallic and non-metallic structures in the aerospace, sports, construction, petroleum and oil industry [1-2]. The fiber reinforced polymer (FRP) matrix composite repair system is widely used for metallic pipelines in offshore and onshore units as it offers many advantages such as: corrosion prevention, quick repair, cold work, safety and it is more economical etc. over a conventional welding repair method [3-7]. An assessment of a composite repair system for corroded pipelines is in progress and many researchers carried out hydrostatic testing of metallic pipelines reinforced with composites to assure the structural integrity [8-13]. Generally, hydrostatic tests are performed according to the ASME PCC-2 [14] and ISO/TS 24817 [15] composite repair standards. Still, there is a continuous modification of the standard over a theoretical failure pressure prediction with the input from the research studies [16-21].

Several theoretical models have been proposed on corroded pipelines reinforced with a polymer based composite repair system under certain assumptions and were also validated with the hydrostatic test results [22-26]. Many proposed models predicted a reasonably accurate failure pressure but still there is a difference between the theoretical and the experimental failure pressures. This difference is caused by many assumptions while deriving the expression, such as, neglecting axial and radial stresses and not accounting for the plastic deformation far away from the defect region. These assumptions help to derive a simple expression to predict the failure pressure using only the elastic properties of the materials but at the cost of low accuracy. Besides the composite material properties, the fiber orientation, stacking sequence, fiber placement, repair thickness, lay-up angle, material behavior model are the important parameters for a pipe, where the stresses are generated along circumferential and axial directions [27-29]. A sensitivity analysis was performed to identify the effect of these parameters and optimize the composite system for better performance and reliability of the composite structure also studied [27, 28]. Many authors [22-24, 30] suggested to account for these assumptions for a more accurate prediction of the failure pressure but still have not accounted for it in the analysis, because of the complexity in the analytical expressions. In addition to these assumptions, the remaining strength and flow stress parameters are the possible causes for the difference in the theoretical and experimental failure pressures, which varies as per selection criterion. There are many available criteria listed in the literature and the most commonly used criteria are ASME B31G, RSTENG 0.85, DNV and their modified version along with Ritchie and last, RC/Battelle, Chell, Sims, Kanninem and Chell [17, 31-36].

The Failure analysis of corroded metallic pipelines reinforced with a polymer based composite repair system is well developed but considered only the circumferential stress and neglected the axial and radial stresses [17]. The axial stress is neglected due to the fact that the real pipeline is open at both ends and is very long, however hydrostatic tests are usually performed taking as cylindrical specimen closed at both ends. In the present work the problem is modelled in the context of elasto-plasticity as a thin-walled cylinder closed at the extremities (axial stress) to predict an accurate failure pressure. The material behavior is assumed to be elastic far from the defect region. In order to validate the effectiveness of the proposed methodology, the failure pressures obtained in a series of hydrostatic tests of pipes are compared with the theoretical failure pressure [4, 20, 24, 25]. Furthermore, the failure pressure is calculated by using different criteria and compared with the experimental results, in order to find the best criterion to be used based on the requirement of accuracy and conservative level.

2. Thin-walled elastic-plastic pipe under internal pressure

The aim of this study is to propose a theoretical analysis constrained to thin-walled metallic pipes and considering a set of elastic-plastic constitutive equations to predict failure pressure. The idea is to obtain an analytical expression which can account for a more practical condition such as the pipe specimen extremities, variation of the thickness and localized plastic deformation in order to predict a more accurate failure pressure.

It is considered an elasto-plastic cylinder with internal radius (r_i), pipe thickness (e), subjected to an internal pressure (P_i) (Fig. 1).

$$\frac{r_i}{e} > 10 \quad \text{Thin-wall cylinder condition} \tag{1}$$

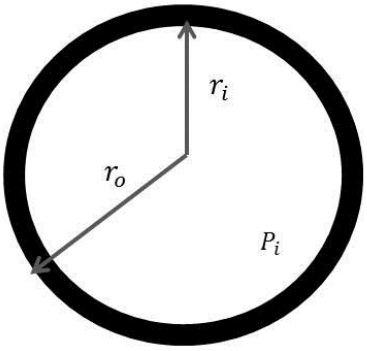

Fig. 1. Pipe with internal pressure.

The stress component of the thin-walled cylinder in the cylindrical co-ordinate system *(r-θ-z)* is as shown below:

$$\sigma = \begin{bmatrix} \sigma_r & 0 & 0 \\ 0 & \sigma_\theta & 0 \\ 0 & 0 & \sigma_z \end{bmatrix} \tag{2}$$

Where, σ_r, σ_θ and σ_z are the radial, circumferential and axial stress components of the cylinder, while the shear stresses $\tau_{r\theta}, \tau_{\theta z}$ and τ_{rz} are neglected as they are relatively negligible compared to the normal stress components.

Considering a thin-walled isotropic cylinder and that the radial stress along the radial direction is constant ($\sigma_r = 0$), equation (2) becomes:

$$\sigma = \begin{bmatrix} \sigma_r = 0 & 0 & 0 \\ 0 & \sigma_\theta & 0 \\ 0 & 0 & \sigma_z = \sigma_\theta/2 \end{bmatrix} \text{ for a closed cap cylinder } (\sigma_z \neq 0) \tag{3}$$

$$\sigma = \begin{bmatrix} \sigma_r = 0 & 0 & 0 \\ 0 & \sigma_\theta & 0 \\ 0 & 0 & \sigma_z = 0 \end{bmatrix} \text{ for an open cap cylinder } (\sigma_z = 0) \tag{4}$$

With, $\sigma_\theta = \frac{Pr_i}{e}$ and $\sigma_z = \frac{\sigma_\theta}{2} = \frac{Pr_i}{2e}$ (5)

Generally, the axial stress is assumed to be negligible for long pipes but it becomes influential when closed on both sides during a hydrostatic test. The axial stress in a closed pipe is almost half of the circumferential stress, so both stress components are dependent $\left(\sigma_z = \frac{\sigma_\theta}{2}\right)$ to each other.

Considering the plastic deformation behavior of the pipe, the tangential stress becomes:

$$\sigma_\theta = \sigma_y + K(\varepsilon_\theta^p)^N \text{if} \quad \sigma_\theta > \sigma_y \tag{6}$$

Where, σ_y is the yielding stress, K and N are the positive material constants that characterize the plastic behavior of the material. If, $\sigma_\theta < \sigma_y$ it means no plastic deformation occurs, ε_θ^p=0.

The total strain of the pipe material is as follows:

$$\varepsilon_\theta = \varepsilon_\theta^e + \varepsilon_\theta^p = \frac{\sigma_\theta}{E} + \varepsilon_\theta^p \tag{7}$$

Assuming that, $\varepsilon_\theta \approx \frac{u_r}{r_i}$

The radial displacement can be obtained through equation (8):

$$\frac{u_r}{r_i} = \frac{\sigma_\theta}{E} + \left(\frac{\sigma_\theta - \sigma_y}{K}\right)^{1/N} \tag{8}$$

The radial displacement u_r for the elastic-plastic behavior can be expressed as:

$$u_r = r_i\left[\frac{\sigma_\theta}{E} + \left(\frac{\sigma_\theta - \sigma_y}{K}\right)^{1/N}\right] \tag{9}$$

While, the radial displacement for the elastic behavior can be expressed as:

$$u_r = r_i\left(\frac{\sigma_\theta}{E}\right) \tag{10}$$

There are two classical yield failure criteria: the Tresca criterion and the von Mises criterion which are used extensively in structural stresses and deformation analysis. In this study, the von Mises failure criterion is used to predict the theoretical failure pressure with accounting for the circumferential and axial stresses. The Principal stresses σ_1 (σ_z), σ_2 (σ_θ) and σ_3 (σ_r) are acting on the thin walled cylinder subjected to internal pressure as shown in Fig. 2.

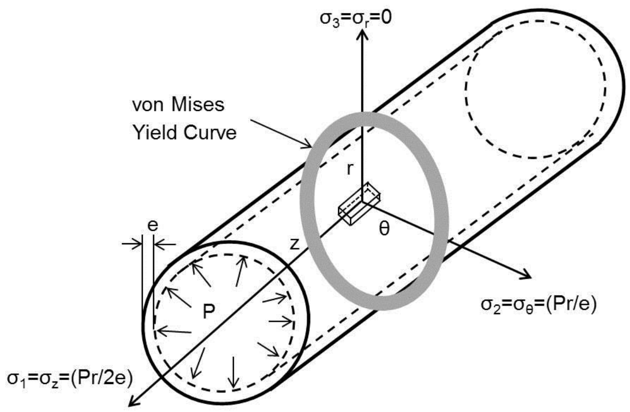

Fig. 2. Principal stresses on thin pressurized cylinder with closed end caps.

As per the definition of the von Mises yield failure criterion, the general form of the von Mises failure criterion in terms of principal stresses is:

$$\frac{1}{\sqrt{2}}[(\sigma_1-\sigma_2)^2+(\sigma_2-\sigma_3)^2+(\sigma_3-\sigma_1)^2]^{1/2}=\sigma_y \tag{11}$$

The plane stress (thin cylinder), $\sigma_3\ (\sigma_r)=0$, therefore, the von Mises criterion for cylindrical coordinates *(r-θ-z)*, assuming that the radial stress is zero, $\sigma_r=0$, yields equation (12):

$$[(\sigma_\theta)^2-(\sigma_\theta\sigma_z)+(\sigma_z)^2]^{1/2}=\sigma_y \tag{12}$$

The above equation is valid, if the pipe is closed, which confirms the presence of an axial stress term in the analysis, otherwise for the open ended cylinder condition $(\sigma_z=0)$, equation (12) reduces to:

$$\sigma_\theta=\sigma_y \tag{13}$$

This form is the most used as it is simple and easy to formulate the mathematical expression for the failure pressure of a damaged pipe and it gives a more conservative failure value as it considers only the circumferential stress.

The internal failure pressure for the cylinder with elastic behavior is:

$$\sigma_\theta=\sigma_y=\frac{Pr_i}{e} \tag{14}$$

$$P=\frac{(e\sigma_y)}{r_i} \tag{15}$$

The maximum theoretical failure pressure can be related to the ultimate stress, σ_{ult}, as it was explained in [22, 23].

$$P_{max}^{th}=\frac{(e*\sigma_{ult})}{r_i} \tag{16}$$

3. Remaining strength criteria for wall loss defects (α_θ)

The wall loss defect in metallic pipes is taken into account by the remaining strength factor (damage factor). This factor (α_θ) is a function of defect and pipe geometry and varies according to the selection criteria. All these criteria can be expressed as follows:

$$\sigma_\theta=\alpha_\theta\left(\frac{P_ir_i}{e}\right)_{undamaged} \tag{17}$$

The maximum theoretical failure pressure of the wall loss defect of a metallic pipeline can be determined as:

$$P_{max}^{th} = \frac{e}{\alpha_\theta r_i}\sigma_{flow} \tag{18}$$

Where, α_θ is the damage factor and σ_{flow} is the maximum allowable strength before failure, both parameters vary according to the criterion. ASME B31G and RSTRENG 0.85 criteria are the most widely used for corroded pipelines subjected to an internal pressure [17, 32-35]. The difference between the many criteria is the option of the flow stress and the expression for the remaining strength factor, so careful selection of criterion is needed. The remaining strength factor and flow stress formulae of ASME B31G, RSTRENG and DNV and the modified version of each criterion are listed in Table. 1. The most widely used criteria are ASME B31G, RSTRENG 0.85 and DNV and their modified version, as these criteria predict a more accurate failure pressure than other criteria [17, 24, 25].

Table 1 Criterion for remaining strength factor and flow stress equation

Criteria	Remaining strength factor (α_θ)	Bulging Factor	Flow stress
ASME B31G [34, 36]	$If\ A_f \le 4,\quad \alpha_\theta = \frac{1-\frac{2}{3}\left(\frac{d}{e\sqrt{A_f^2+1}}\right)}{1-\frac{2}{3}\left(\frac{d}{e}\right)}$ $If A_f > 4\ ,\quad \alpha_\theta = \frac{e}{e-d}$	$A_f = 0.893\left(\frac{L}{\sqrt{De}}\right)$	$\sigma_{flow} = 1.1\sigma_y$
ASME B31G* [17, 36]	Same as ASME B1G	Same as ASME B1G	$\sigma_{flow} = \sigma_{ult}$
RSTRENG 0.85 [34, 36]	$\alpha_\theta = \frac{1-0.85\left(\frac{d}{e}\right)\left(\frac{1}{M_t}\right)}{1-0.85\left(\frac{d}{e}\right)}$	$M_t = \sqrt{1+0.275\left(\frac{L^2}{De}\right)-0.00375\left(\frac{L^2}{De}\right.}$ $M_t = 3.3 + 0.032\left(\frac{L^2}{De}\right)$	$\sigma_{flow} = \sigma_y + 69$
RSTRENG 0.85* [17, 36]	Same as RSTRENG 0.85	Same as RSTRENG 0.85	$\sigma_{flow} = \sigma_{ult}$
DNV [17]	$\alpha_\theta = \left[\frac{1-\left(\frac{d}{e}\right)\left(\frac{1}{Q}\right)}{1-\left(\frac{d}{e}\right)}\right]$	$Q_t = \sqrt{1+0.31\left(\frac{L^2}{De}\right)}$	$\sigma_{flow} = \sigma_{ult}$

4. Proposed methodology for failure pressure analysis of composite repair system

The present section is concerned with the analysis of composite sleeve reinforcement systems for metallic pipelines, which accounts for a practical condition such as pipe specimen extremities (closed cap cylinder) for predicting a more accurate failure pressure.

The basic assumption is that the wall loss defect is localized and thus the stress and strain fields far from the defect are not subjected to plastic deformation. As a consequence, the material behavior is assumed to be elastic far from the defect. The behavior of steel pipe at defect section is idealized an elastic-perfectly plastic (without strain hardening of steel). The pipe-composite sleeve system is modelled as two concentric thin-walled cylinders subjected to an internal pressure P_i and contact pressure P_c between the pipe and composite sleeve (Fig. 3). The pipe has an inner radius r_i and external diameter D with defect length L and depth d, while the composite sleeve has an internal radius r_o and external radius r_e (Fig. 4).

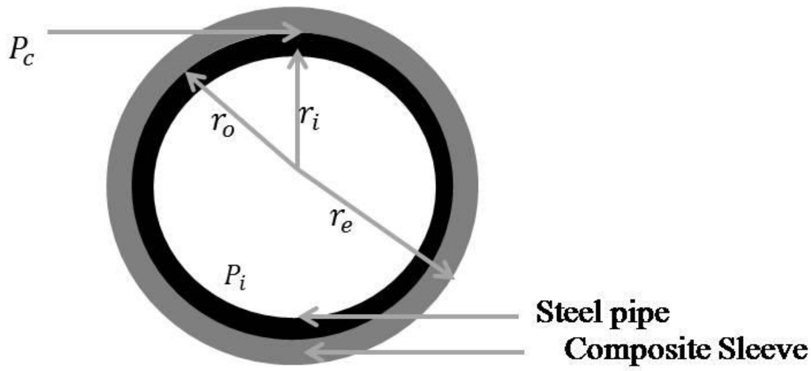

Fig. 3. Pipe and sleeve with internal and contact pressure.

If the wall thickness of a pipe e_{pipe} is less than $1/10^{th}$ of the internal radius of the cylinder, $e_{pipe}=(r_o-r_i)<(r_i/10)$, then the cylinder wall is considered thin, otherwise, it is considered thick [31]. Similarly for the composite sleeve, $e_{sleeve}=(r_e-r_o)<(r_o/10)$.

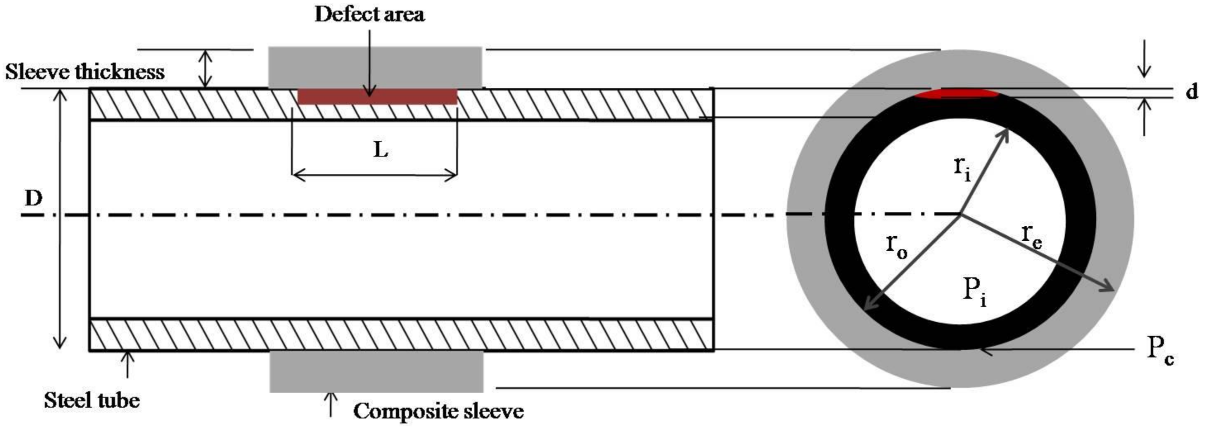

Fig. 4. Metal loss in the pipe with a composite reinforcement sleeve.

Table 2 Hydrostatic burst test data.

Test	Pipe							Composite		P_{max}^{exp}
(Ref)	E_{pipe} (GPa)	σ_{ult} (MPa)	σ_y (MPa)	D (mm)	e_{pipe} (mm)	d (mm)	L (mm)	E_{sleeve} (GPa)	e_{sleeve} (mm)	(MPa)
1 [20]	210	608	413	508	14.3	10.01	500	20	25	27.9
2 [20]	210	604	413	508	14.3	10.01	500	20	25	26.7
3 [20]	210	600	413	508	14.3	10.01	500	20	25	23.6
4 [20]	210	600	413	508	14.3	10.01	500	20	25	23.5
5 [20]	210	563	413	508	14.3	10.01	500	27	25	19.2
6 [20]	210	563	413	508	14.3	10.01	500	27	25	20.2
7 [20]	210	616	413	508	14.3	10.01	500	27	25	22.8
8 [20]	210	621	413	508	14.3	10.01	500	27	25	23.2
9 [20]	210	605	413	508	14.3	10.01	500	28	25	23.5
10 [20]	210	583	413	508	14.3	10.01	500	28	25	23.4
11 [20]	210	621	413	508	14.3	10.01	500	8	25	19.9
12 [4]	207	474	360	168.3	7.11	3.56	152.4	49	3.10	43.81
13 [4]	207	474	360	168.3	7.11	3.56	152.4	49	3.10	43.1
14 [25]	210	613	360	476.4	9.53	6.7	450	21.7	21.42	14
15 [25]	210	613	450	476.4	9.53	6.7	450	21.7	21.42	14.2
16 [25]	210	613	450	476.4	9.53	6.7	450	21.7	21.42	14.2
17 [24]	210	627	390	168.3	7.11	5.688	86.82	21.21	16.2	36.75
18 [24]	210	627	390	168.3	7.11	5.688	86.82	21.21	16.2	35.19
19 [24]	210	627	390	168.3	7.11	5.688	86.82	21.21	16.2	36.90

The variation of the wall thickness due to the pressure can be neglected, hence the radial displacement u_r can be assumed to be a constant value. Assuming that the radial displacement in the contact surface is the same for both cylinders, it is possible to obtain analytical expressions for the stress, strain and displacement fields. The contact surface between the pipe and the composite sleeve can be approximated using the following relation and correlate with the initial pressure.

[Radial displacement] pipe = [Radial displacement] sleeve

$$[u_r]_{pipe} = [u_r]_{sleeve} \tag{19}$$

$$r_i[\varepsilon_\theta]_{pipe} = r_o[\varepsilon_\theta]_{sleeve} \tag{20}$$

$$r_i \frac{[\sigma_\theta]_{pipe}}{E_{pipe}} = r_o \frac{[\sigma_\theta]_{sleeve}}{E_{sleeve}} \tag{21}$$

$$\frac{r_i}{E_{pipe}}\left(\frac{P_i r_i - P_c r_o}{r_o - r_i}\right) = \frac{r_o}{E_{sleeve}}\left(\frac{P_c r_o}{r_e - r_o}\right) \tag{22}$$

The contact pressure, P_c, acting between the pipe and the composite sleeve (Fig. 4) can be approximated in terms of internal pressure using the following relation:

$$P_c = P_i\left[\frac{(r_0 - r_i)}{(r_e - r_o)}\left(\frac{E_{pipe}}{E_{sleeve}}\right)\left(\frac{r_0}{r_i}\right)^2 + \left(\frac{r_0}{r_i}\right)\right]^{-1} = \beta P_i \tag{23}$$

If the composite repair thickness (e_{sleeve}) is higher than 1/10th of the external radius of the steel tube r_o then, the sleeve's radial displacement cannot be assumed constant. In this case, the equations 19, 22, and 23 becomes:

$$[u_r]_{pipe} = [u_r\,(r = r_o)]_{sleeve} \tag{24}$$

$$\frac{r_i}{E_{pipe}}\left(\frac{P_i r_i - P_c r_o}{r_0 - r_i}\right) = -BP_cKr_o^{-k}\left(\frac{1}{E_{\theta\theta}} + \frac{\nu_{r\theta}}{E_{rr}}\right) + CP_cKr_o^{k}\left(\frac{1}{E_{\theta\theta}} - \frac{\nu_{r\theta}}{E_{rr}}\right) \tag{25}$$

$$P_c = \frac{\dfrac{r_i^2}{E_{pipe}(r_i - r_o)}}{-BKr_o^{-k}\left(\frac{1}{E_{\theta\theta}} + \frac{\nu_{r\theta}}{E_{rr}}\right) + CKr_o^{k}\left(\frac{1}{E_{\theta\theta}} - \frac{\nu_{r\theta}}{E_{rr}}\right) + \frac{r_i\, r_o}{E_{pipe}(r_i - r_o)}} P_i = \beta P_i \tag{26}$$

Where, $K = \sqrt{\frac{E_\theta}{E_r}}$, $B = \left(\frac{r_e^{K-1}}{\left[r_o^{-(K+1)} r_e^{(K-1)} - r_o^{(K+1)} r_e^{-(K-1)}\right]}\right)$, $C = \left(\frac{r_e^{-(K-1)}}{\left[r_o^{-(K+1)} r_e^{(K-1)} - r_o^{(K+1)} r_e^{-(K-1)}\right]}\right)$

Let us consider the axial stress component (test pipe extremities) in the failure pressure analysis that is not accounted in previous studies. Usually, the hydrostatic tests are performed considering a cylindrical specimen closed at the both ends using a welded cap or a bolted pressure flange. However, in reality, the pipeline is not closed, therefore, the effect of axial stresses in the longitudinal direction is almost negligible. In the present analysis the problem is modelled in the context of elasto-plasticity as a thin-walled cylinder closed at the extremities. To account for the effect of a closed cap pipe (pipe extremities condition) in the final failure pressure, both the circumferential (hoop) and axial stresses are considered for the determination of the failure pressure.

$$\text{Circumferential stress } (\sigma_\theta) = \left(\frac{P_i r_i - P_c r_o}{r_o - r_i}\right) = \left(\frac{P_i r_i - P_c r_o}{e}\right) \tag{27}$$

$$\text{Axial stress } (\sigma_z) = \frac{\sigma_\theta}{2} = \left(\frac{P_i r_i - P_c r_o}{2*(r_o - r_i)}\right) = \left(\frac{P_i r_i - P_c r_o}{2*e}\right) \tag{28}$$

As per the definition of the von Mises failure criterion, considering the circumferential and axial stresses on the cylinder, the failure criterion is reduced to:

$$(\sigma_\theta)^2 - (\sigma_\theta \sigma_z) + (\sigma_z)^2 = \sigma_y^2 \tag{29}$$

Substituting the circumferential and axial stresses of the metallic pipeline reinforced with a composite sleeve in the above equation:

$$\left(\frac{P_i r_i - P_c r_o}{e}\right)^2 - \left(\frac{P_i r_i - P_c r_o}{e}\right) * \left(\frac{P_i r_i - P_c r_o}{2e}\right) + \left(\frac{P_i r_i - P_c r_o}{2e}\right)^2 = \sigma_y^2 \tag{30}$$

$$\frac{3P_i^2 * r_i^2}{4e^2} - \frac{3P_i r_i * P_c r_o}{2e^2} + \frac{3P_c^2 * r_o^2}{4e^2} = \sigma_y^2 \tag{31}$$

To calculate the failure pressure of the pipe with a composite sleeve, there is a need to consider the ultimate stress, but for a safer design the yield stress would be preferable. Several researchers [22-24] have already related failure pressure P_{max} with the ultimate stress (σ_{ult}) from a tensile test but generalized in terms of the flow stress (σ_{flow}) and the values are different depending on the selection of the remaining strength criteria.

$$\frac{3P_i^2 * r_i^2}{4e^2} - \frac{3P_i r_i * P_c r_o}{2e^2} + \frac{3P_c^2 * r_o^2}{4e^2} = \sigma_{flow}^2 \tag{32}$$

From equation (23), $P_c = \beta P_i$, therefore, equation (32) becomes:

$$\left(\frac{3P_i^2 * r_i^2}{4e^2} - \frac{3P_i r_i * \beta P_i r_o}{2e^2} + \frac{3(\beta P_i)^2 * r_o^2}{4e^2}\right) = \sigma_{flow}^2 \tag{33}$$

It is possible to obtain the theoretical failure pressure, P_f^{th} as:

$$\left(P_f^{th}\right)^2 \left(\frac{3r_i^2}{4e^2} - \frac{3\beta r_i r_o}{2e^2} + \frac{3\beta^2 r_o^2}{4e^2}\right) = \sigma_{flow}^2 \tag{34}$$

$$P_{max}^{th} = \frac{\sigma_{flow}}{\sqrt{k_1}} \quad \text{Where } k_1 = \left(\frac{3r_i^2}{4e^2} - \frac{3\beta r_i r_o}{2e^2} + \frac{3\beta^2 r_o^2}{4e^2}\right) \tag{35}$$

To account for a localized defect section in the pipe a damage factor (α_θ) is introduced, therefore, the failure pressure of the metal wall loss defect pipe corrected by the factor α_θ is:

$$P_{max}^{th} = \frac{\sigma_{ult}}{\alpha_\theta \sqrt{k_1}} \tag{36}$$

On the other hand, without accounting for the axial stress, the failure criterion (von Mises) equation (29) is reduced to:

$$\sigma_\theta = \sigma_y \tag{37}$$

From equation (27), the above equation becomes:

$$\left(\frac{P_i r_i - P_c r_o}{r_o - r_i}\right) = \sigma_y \tag{38}$$

As we know, $P_c = \beta P_i$, therefore:

$$\left(\frac{P_i r_i - \beta P_i r_o}{e}\right) = \sigma_y \tag{39}$$

Thus, for the maximum theoretical failure pressure the yield stress becomes the ultimate stress of the pipe:

$$P_{max}^{th} \left(\frac{r_i - \beta r_o}{e}\right) = \sigma_{ult} \tag{40}$$

$$P_{max}^{th} = \frac{\sigma_{ult}}{k_2}, \quad \text{Where } k_2 = \left(\frac{r_i - \beta r_o}{e}\right) \tag{41}$$

$$P_{max}^{th} = \frac{\sigma_{ult}}{\alpha_\theta k_2} \tag{42}$$

A total of 19 hydrostatic tests results are considered from different laboratories, including 3 hydrostatic tests results from our laboratory in order to validate the proposed methodology with and without accounting for the axial stress using different criterion [4, 20, 24-25]. Table 2 summarizes the geometrical and material properties of damaged pipelines reinforced with composites, as well as the experimental failure pressure of the tested specimens [4, 20, 24-25]. As per the present methodology, only geometric and material properties of damaged pipelines and composite repair systems are required to calculate the theoretical failure pressure. The theoretical failure pressure is calculated based on different criteria: ASME B31G, RSTRENG 0.85 and their modified version and DNV subjected with and without axial stress are listed in Table 3. The theoretical failure pressure obtained from the proposed models is higher and closer towards the experimental failure pressure than the previous model without accounting for the axial stress [17].

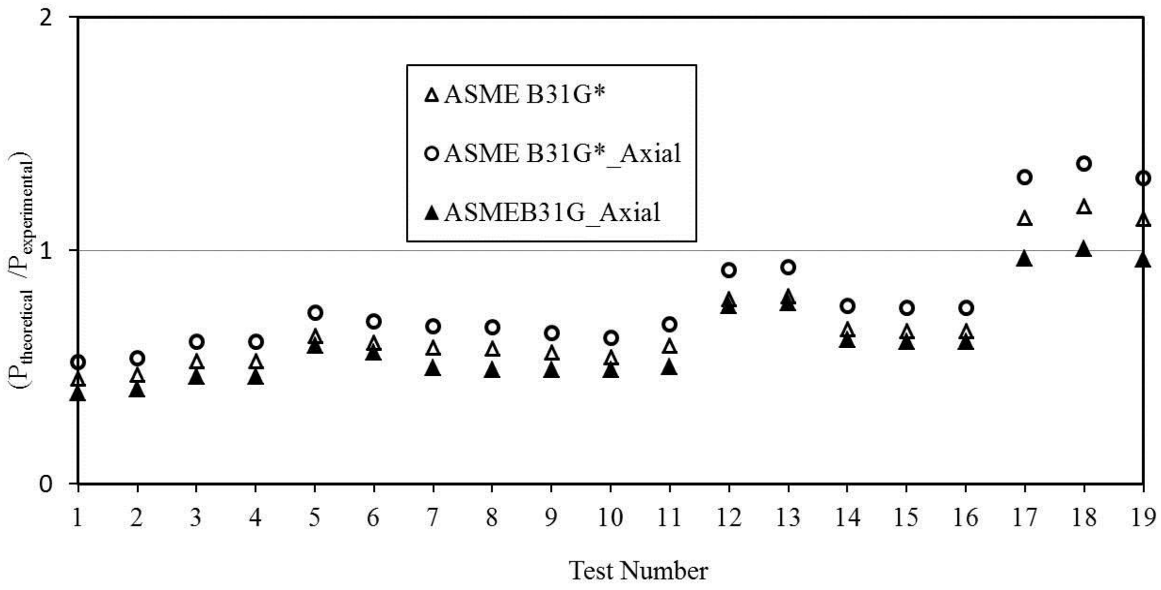

Fig. 5. ($P_{theoretical}/P_{experimental}$) per test with and without accounting for the axial stress using ASME B31G* criterion.

Table 3 Failure pressure prediction.

Test	P_{max}^{exp} MPa)	Failure pressure P_{max}^{th} (MPa) Without accounting axial stress			Failure pressure P_{max}^{th} (proposed methodology) (MPa) With accounting axial stress				
		ASME B31G*	RSTRENG0.85*	DNV	ASME B31G	RSTRENG 0.85	ASME B31G*	RSTRENG 0.85*	DNV
1	27.9	12.59	17.56	15.84	10.86	16.07	14.54	20.28	18.29
2	26.7	12.51	17.44	15.73	10.86	16.07	14.44	20.14	18.17
3	23.6	12.43	17.33	15.63	10.86	16.07	14.35	20.01	18.05
4	23.5	12.43	17.33	15.63	10.86	16.07	14.35	20.01	18.05
5	19.2	12.21	17.03	15.36	11.38	16.84	14.10	19.67	17.74
6	20.2	12.21	17.03	15.36	11.38	16.84	14.10	19.67	17.74
7	22.8	13.36	18.64	16.81	11.38	16.84	15.43	21.52	19.41
8	23.2	13.47	18.79	16.94	11.38	16.84	15.56	21.69	19.57
9	23.5	13.21	18.42	16.61	11.45	16.95	15.25	21.27	19.18
10	23.4	12.73	17.75	16.01	11.45	16.95	14.70	20.50	18.49
11	19.9	11.81	16.47	14.86	9.98	14.76	13.64	19.02	17.16

12	43.8	34.73	28.50	29.46	33.50	29.78	40.10	32.91	34.01
13	43.1	34.73	28.50	29.46	33.50	29.78	40.10	32.91	34.01
14	14.0	9.28	12.92	11.35	8.65	12.63	10.71	14.92	13.11
15	14.2	9.28	12.92	11.35	8.65	12.63	10.71	14.92	13.11
16	14.2	9.28	12.92	11.35	8.65	12.63	10.71	14.92	13.11
17	36.75	41.88	26.21	26.43	35.47	26.25	48.36	30.27	30.52
18	35.19	41.88	26.21	26.43	35.47	26.25	48.36	30.27	30.52
19	36.90	41.88	26.21	26.43	35.47	26.25	48.36	30.27	30.52

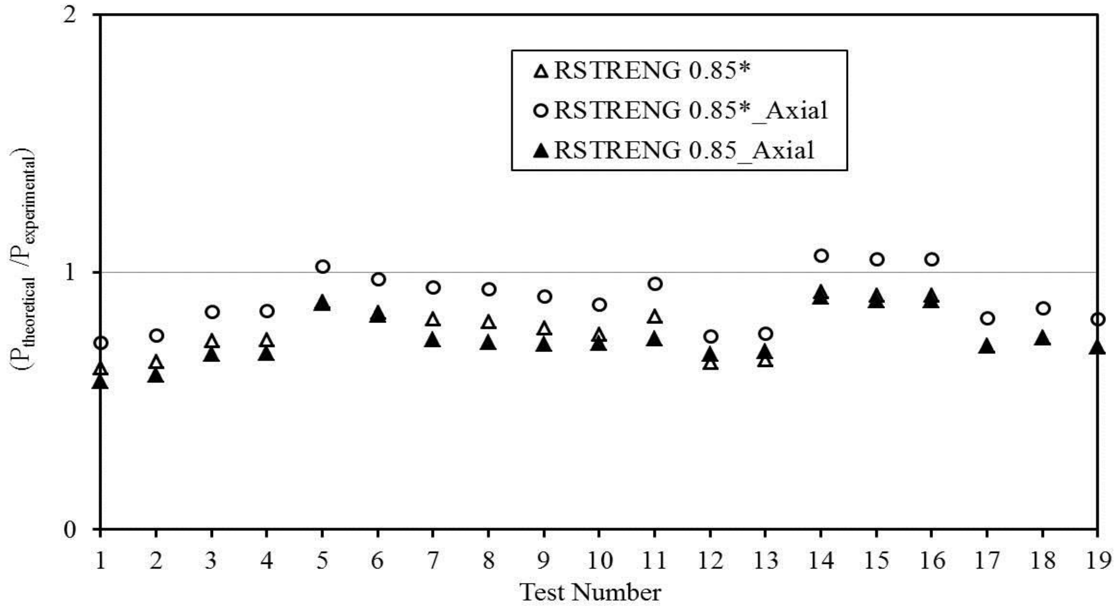

Fig. 6. ($P_{theoretical}/P_{experimental}$) per test with and without accounting for the axial stress using RSTRENG 0.85* criterion.

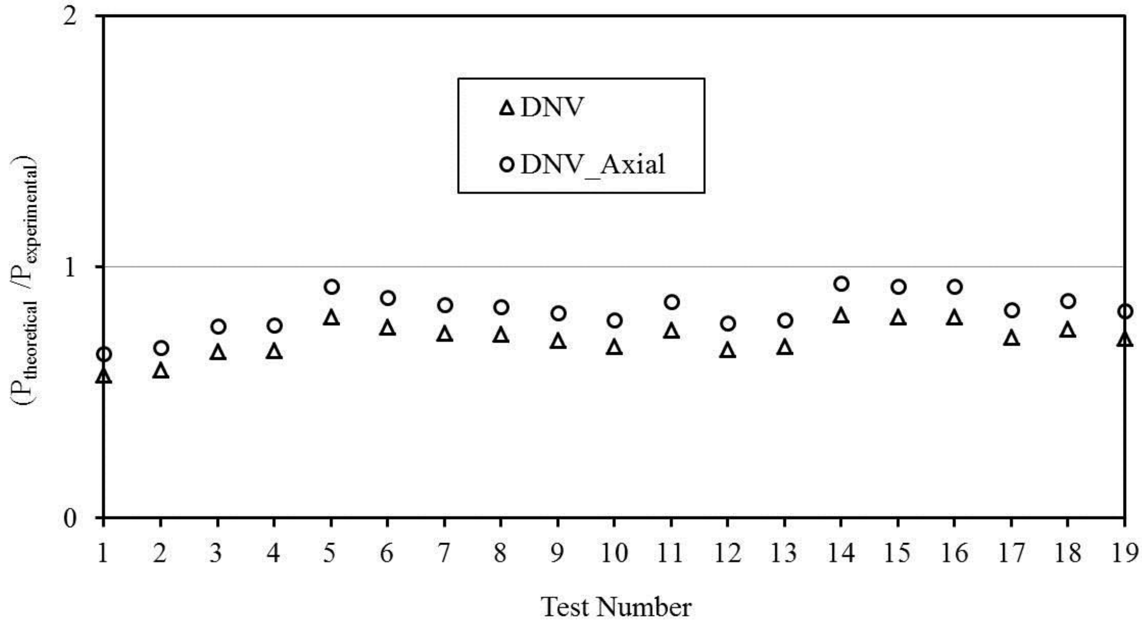

Fig. 7. ($P_{theoretical}/P_{experimental}$) per test with and without accounting for the axial stress using DNV criterion.

Figures 5-7 show the ratio between the predicted theoretical failure pressure and the experimental failure pressure ($P_{theoretical}/P_{experimental}$) with and without accounting for the axial stress using the criteria ASME B31G, RSTRENG 0.85, DNV and their modified version.

The predicted failure pressure with accounting for the specimen extremities (axial stress) is more accurate than without the axial stress in all criteria except in some cases. Based on the three criteria, the DNV criterion shows an accurate prediction as well as reasonable and conservative for all tested specimens, while the RSTRENG 0.85* criterion is more accurate and closer to experimental values but over-predicted in some tests. Most of the conservative values of failure pressure are obtained under the ASME B31G and RSTRENG 0.85 criterion rather than the other criteria (ASME B31G*, RSTRENG 0.85* and DNV), the same trend was also noticed by other researchers [17, 24].

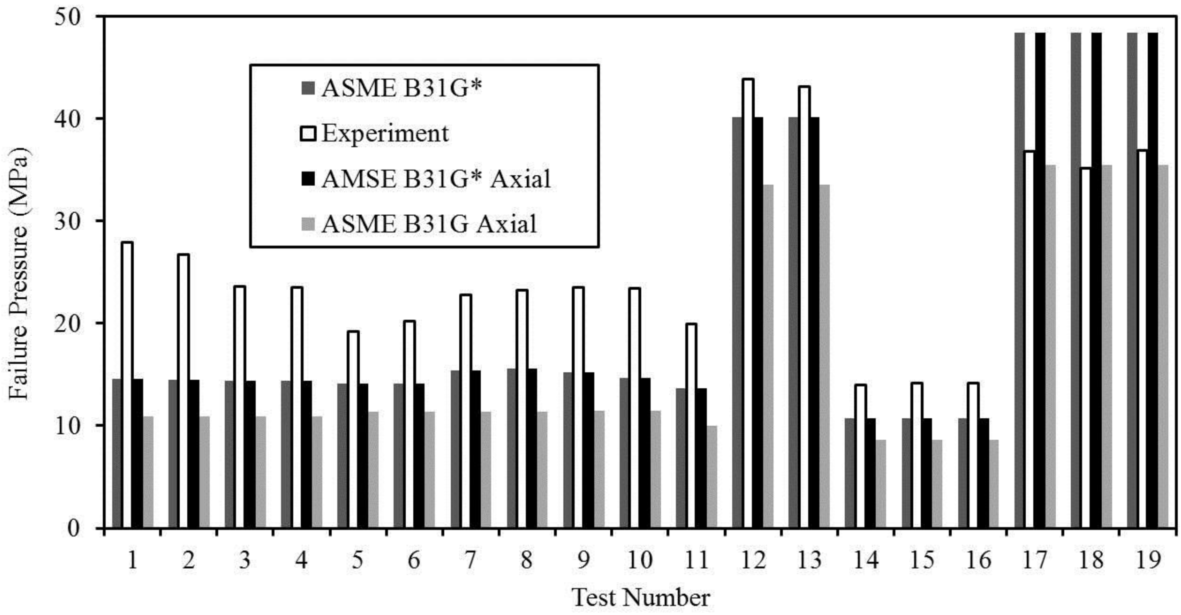

Fig. 8. Comparison between predicted and experimental failure pressure for different conditions using ASME B31G criterion.

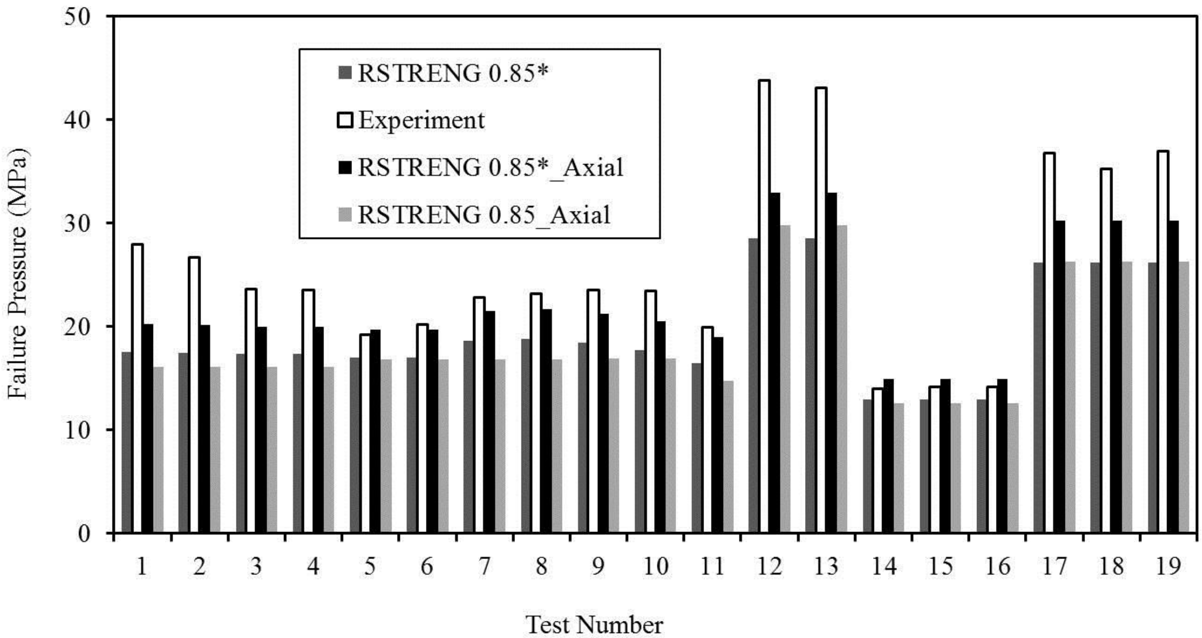

Fig. 9. Comparison between predicted and experimental failure pressure for different conditions using RSTRENG 0.85 criterion.

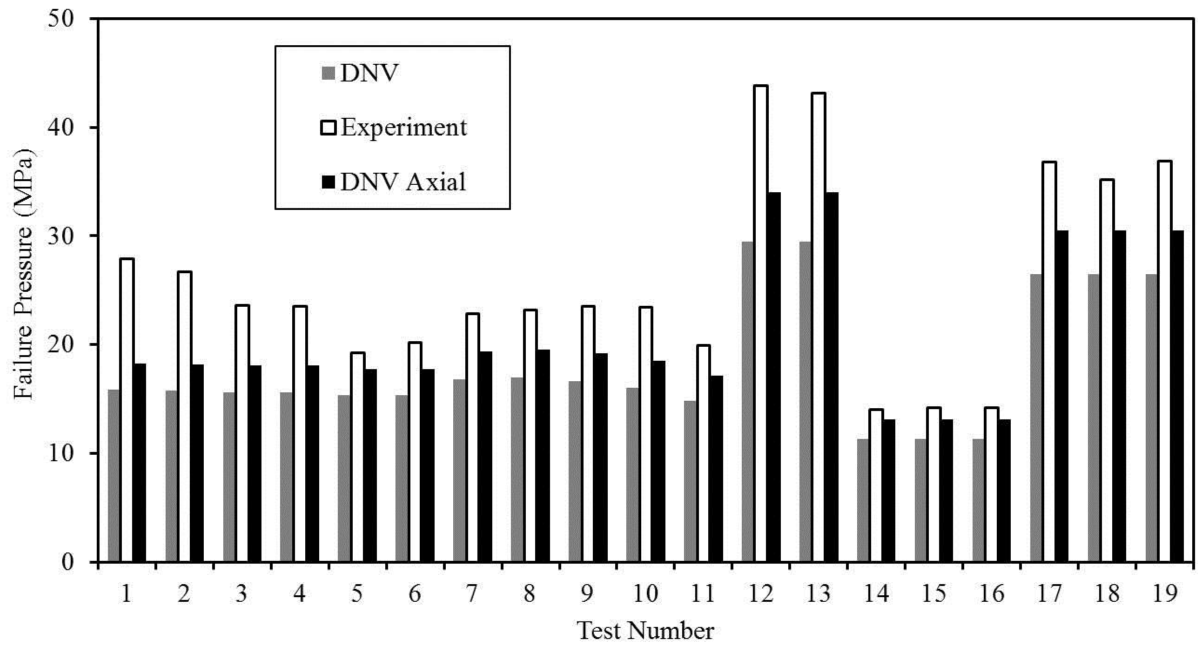

Fig. 10. Comparison between predicted and experimental failure pressure for different conditions using DNV criterion.

Figures 8-10 show the comparison between the experimental failure pressure and the predicted theoretical failure pressure with and without accounting for the axial stress using different criteria. The failure pressure with accounting for the axial stress in the proposed model predicted a higher failure pressure than without axial stress for all criteria and is closer towards the experimental failure pressure but in some cases, it over-predicted for the ASME B31G* and RSTRENG 0.85* but not for the DNV criterion. The DNV criterion predicted an accurate and conservative failure pressure in all experiment tests but a more accurate prediction was obtained when the proposed methodology accounted for the axial stress. The proposed analysis, which accounts for the test specimen extremities (axial stress) shows more accurate results and requires properties of the pipe and the composite sleeve. All three criteria ASME B31G, RSTRENG 0.85, DNV and their modified version (ASME B31G*, RSTRENG 0.85*) have different failure pressure values in the proposed method, as it depends on the remaining strength factor and flow stress condition. From mixed trends results, it is observed that the pipe test specimen geometry and material properties also play an important role. Therefore, proper selection of criteria is necessary, as per the area of application and requirement of accuracy and conservative level of failure pressure.

Still, there is a difference between the theoretical failure pressure using the proposed methodology and the experimental failure pressure and this difference can be minimized by accounting for the plastic deformation of the pipe, variation of the thickness of the composite sleeve (radial stress) etc. as suggested by researchers [23, 24, 30, 31]. In the previous experimental study [12], the plastic deformation occurs far from the defect region, hence this phenomenon needs to be accounted for in the analysis for a more accurate prediction (Fig.11). Plastic deformation occurs at 85 mm distance away from the end of the defect region in both sides of the tube (left and right). There is scope to refine this proposed analysis by introducing the plastic deformation phenomenon with the cost of a more complex analytical equation and material properties under plastic deformation.

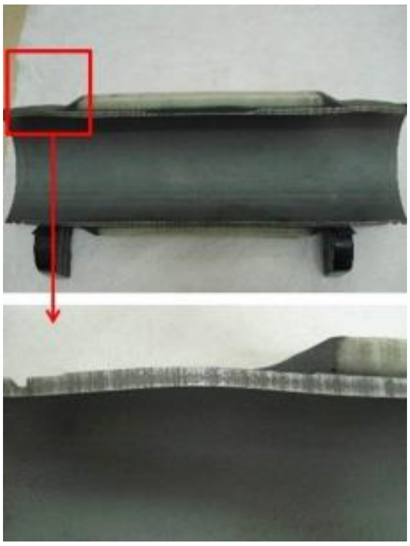

Fig. 11. Tube deformation during hydrostatic test [12].

5. Conclusions

The present paper proposed a simple methodology to estimate the failure pressure of corroded pipelines reinforced with a composite sleeve. In this methodology, the metallic pipe extremities (closed end cap) were accounted for in the analysis, which is similar to the hydrostatic test specimen condition in order to predict a more accurate failure pressure. With a simple expression, a realistic estimate for the failure pressure of a corroded thin-walled pipe reinforced with a composite sleeve can be obtained. The estimation of the failure pressure requires only the knowledge of the properties of the pipe and composite sleeve, along with pipe specimen geometry. This methodology can also be used to define the composite repair thickness in order to assure a reliable operation under a defined pressure.

A total of 19 hydrostatic test results were validated with the proposed methodology. The correlation between the model prediction and the experimental failure pressure is good in most of the cases, which encourages the use of the model as a preliminary tool in the design/analysis of a composite repair system for damaged pipelines. The failure pressure calculated based on the proposed model with accounting for the pipe extremities (axial stress) is more accurate than the one that does not. Both accuracy and conservative level depends on the selection of criteria, for example ASME B31G is more conservative while RSTRENG 0.85* is more accurate but in some experiments it over-predicted, while the DNV criterion perfectly fit in terms of accuracy and conservativeness. Therefore, a careful selection of the remaining strength criteria based on the safety level and other factors is necessary. This new proposed methodology estimated more accurate results, but can still be refined with accounting for the radial stress and the fact that the plastic deformation of the tube occurs far from the defect region in the failure analysis.

Acknowledgements

Authors would like to acknowledge the support of the Brazilian Research Agencies CNPq, CAPES and FAPERJ.

Conflict of Interest

The authors declare that they have no conflict of interest.

References:

1. M. D. Banea and L. F. M. da Silva, Adhesively bonded joints in composite materials - An Overview, Proc. IME J Mate. Des. Appl., Vol 223, 2009, p 1-18.
2. S. Budhe, M. D. Banea, S. de Barros and L. F. M. da Silva, An updated review of adhesively bonded joints in composite materials, Int. J. Adhes. Adhes., Vol 72, 2017, p 30-42.
3. M. Shamsuddoha, M. M. Islama, T. Aravinthan, A. Manalo, and K. Lau, Effectiveness of using fibre-reinforced polymer composites for underwater steel pipeline repairs, Compos. Struct., Vol 100, 2013, p 40-54.

4. J. Duell, J. Wilson and M. Kessler, Analysis of a carbon composite over wrap pipeline repair system, Int. J. Pres. Ves. Pip., Vol 85, 2008, p 782-788.
5. J. Cuthill, Advances in materials, methods, help gain new users, Pipeline Gas J., Vol. 229 (No.11), 2002, p 64-66.
6. K. B. Armstrong, W. Cole, and G. Bevan, Care and repair of advanced composites, 2nd ed., SAE International, 2005 (London).
7. G. Marsh, Composites renovate deteriorating sewers, Reinforced Plast., Vol 48 (No. 6), 2004, p 20-24.
8. C. Alexander, and O. O. Ochoa, Extending onshore pipeline repair to offshore steel risers with carbon-fiber reinforced composites, Compos Struct., Vol 92, 2010, p 499-507.
9. T. S. Mally, A. L. Johnston, M. Chann, R. H. Walker, and M. W. Seller, Performance of a carbon-fiber/epoxy composite for the underwater repair of pressure equipment, Compos. Struct., Vol 100, 2013, p 542-547.
10. L. Mazurkiewicz, M. Tomaszewski, J. Malachowski, K. Sybilski, M. Chebakov, M. Witek, P. Yukhymets, and R. Dmitrienko, Experimental and numerical study of steel pipe with part-wall defect reinforced with fibre glass sleeve, Int. J. Pres. Ves. Pip., Vol 149, 2017, p 108-119.
11. N. R. F. Rohem, L. J. Pacheco, S. Budhe, M. D. Banea, E. M. Sampaio, and S. de Barros, Development and qualification of a new polymeric matrix laminated composite for pipe repair. Compos. Struct., Vol 152, 2016, p 737-745.
12. L. P. Djukic, W. S. Sum, K. H. Leong, W. D. Hillier, T. W. Eccleshall, and A. Y. L. Leong, Development of a fibre reinforced polymer composite clamp for metallic pipeline repairs, Mater. Des., Vol 70, 2015, p 68-80.
13. M. Salem, B. Mechab, M. Berrahou, B. B. Bouiadjra, and B. Serier, Failure Analyses of Propagation of Cracks in Repaired Pipe Under Internal Pressure, J. Fail. Anal. and Preven., Vol 19, 2019, p 212-218.
14. "Petroleum, petrochemical and natural gas industries-Composite repairs for pipework-Qualification and design, installation, testing and inspection," ISO 24817, ISO, 2006.
15. "Repair of pressure equipment and piping," ASME PCC-2, ASME American Society of Mechanical Engineers, 2011.
16. H. Toutanji, and S. Dempsey, Stress modeling of pipelines strengthened with advanced composite material, Thin Wall Struct., Vol 39, 2011, p 153-165.

17. H. S. da Costa Mattos, J. M. L. Reis, L. M. Paim, M. L. da Silva, R. Lopes, and V. A. Perrut, Failure analysis of corroded pipelines reinforced with composite repair systems. Eng. Fail. Anal., Vol 56, 2016, p 223-236.
18. N. Saeed, H. Ronagh, and A. Virk, Composite repair of pipelines, considering the effect of live pressure-analytical and numerical models with respect to ISO/TS 24817 and ASME PCC-2, Compos. Part B-Eng., Vol 58, 2014, p 605-610.
19. J. L. F. Freire, R. D. Vieira, J. L. C. Diniz, and L. C. Meniconi, Applications of experimental techniques in the field of pipeline integrity series - part 7: effectiveness of composite repairs applied to damaged pipeline, Exp. Tech., Vol 31, 2007, p 59-66.
20. M. F. Köpple, S. Lauterbach, and W. Wagner, Composite repair of through-wall defects in pipework-analytical and numerical models with respect to ISO/TS24817, Compos. Struct., Vol 95, 2013, p 173-178.
21. A. P. Teixeira, C. Guedes Soares, T. A Netto, and S. F. Estefen, Reliability of pipelines with corrosion defects, Int. J. Pres. Ves. Pip., Vol 85, 2008, p 228-237.
22. H. S. da Costa Mattos, L. M. Paim, and J. M. L. Reis, Analysis of burst tests and long-term hydrostatic tests in produced water pipelines, Eng. Fail. Anal., Vol 22, 2012, p 128-140.
23. H. S. da Costa Mattos, J. M. L. Reis, R. F. Sampaio, and V. A. Perrut, An alternative methodology to repair localized corrosion damage in metallic pipelines with epoxy resins. Mater. Des., Vol 30, 2009, p 3581-3591.
24. S. Budhe, M. D. Banea, N. R. F. Rohem, E. M. Sampaio, and S. de Barros, Failure pressure analysis of composite repair system for wall loss defect of metallic pipelines. Compos. Struct., Vol 176, 2017, p 1013-1019.
25. H. S. da Costa Mattos, J. M. L. Reis, L. M. Paim, M. L. da silva, F. C. Amorim, and V. A. Perrut, Analysis of a glass fibre reinforced polyurethane composite repair system for corroded pipelines at elevated temperatures, Compos. Struc., Vol 114, 2014, p 117-123.
26. H. L. D. Cabral, R. S. Motta, S. M. B. Afonso, R. B. Willmersdorf, P. R. M. Lyra, and E. G. de Andrade, The development of a computational tool for generation of high quality FE models of pipelines with corrosion defects, J. Braz. Soc. Mech. Sci. Eng., Vol 39, 2017, p 3137-3150.
27. A. Ghouaoula, A. Hocine, M. Hadj Meliani, A. Maizia, and R. Suleiman, Reliability Analysis of Type III Gas Storage Vessel Under Pressure Loading, J Fail. Anal. and Preven. Vol 19, 20119, p 445-452.

28. A. Hocine, A. Maizia, A. Ghouaoula, and H. Dehmous, Reliability Prediction of Composite Tubular Structure Under Mechanical Loading by Finite Element Method, J Fail. Anal. and Preven. Vol 18, 2018, p 1439-1446.
29. A. Ghouaoula, A. Hocine, D. Chapelle, M. L. Boubakar, and M. Hadj Meliani, Analytical prediction of behaviour of damaged composite tubular structures under quasi-static pressure, Struct. Integrity Life. Vol 18(2), 2018, p 143-148.
30. M. L. da Silva and H.S. da Costa Mattos, Failure pressure estimations for corroded pipelines, Mater. Sci., Vol 759, 2013, p 65-76.
31. S. Budhe, M. D. Banea, S. de Barros S, and N. R. F. Rohem, Assessment of failure pressure of a GFRP composite, repair system for wall loss defect in metallic pipelines. Materialwiss Werkstofftech., Vol 49, 2018, p 1-10.
32. D. R. Stephens and R. B. Francini, A review and evaluation of remaining strength criteria for corrosion defects in transmission pipelines, Proceedings of ETCE/OMAE2000 Joint Conference, New Orleans, 2000, p 293-304.
33. “Manual for determining the remaining strength of corroded pipelines, a supplement to ASME B31 code for pressure piping,” ASME B 31G, ASME, 1991.
34. M. L. da Silva and H. S. da Costa Mattos, Prediction of the burst pressure for metallic pipelines with localized corrosion defects, International symposium on solid mechanics, Porte Alegre, 2012, p 1-14.
35. L.Y. Xu and Y. F. Cheng, Reliability and failure pressure prediction of various grades of pipeline steel in the presence of corrosion defects and pre-strain, Int. J. Pres. Ves. Pip., Vol 89, 2012, p 75-84.
36. B. Ma, J. Shuai, J. Wang , and K. Han, Analysis on the Latest Assessment Criteria of ASME B31G-2009 for the Remaining Strength of Corroded Pipelines, J Fail. Anal. and Preven., Vol 11, 2011, p 666-671.